





Mapping out the spin fluctuations in Co-doped LaFeAsO single crystals by NMR

Piotr Lepucki ¹, Raphael Havemann ¹, Adam P. Dioguardi,¹ Francesco Scaravaggi,^{1,2} Anja U. B. Wolter,¹ Rhea Kappenberger,¹ Saicharan Aswartham ¹, Sabine Wurmehl,^{1,2} Bernd Büchner,^{1,2} and Hans-Joachim Grafe ¹

¹*IFW Dresden, Institut für Festkörperforschung, Helmholtzstraße 20, D-01069 Dresden, Germany*

²*Institut für Festkörper- und Materialphysik and Würzburg-Dresden Cluster of Excellence et.qmat, Technische Universität Dresden, D-01062 Dresden, Germany*



(Received 27 November 2020; accepted 3 May 2021; published 25 May 2021)

We determine the phase diagram of LaFe_{1-x}Co_xAsO single crystals by using nuclear magnetic resonance (NMR). Up to a nominal doping of $x = 0.03$, it follows the phase diagram for F-doped polycrystals. Above $x = 0.03$, the F-doped samples become superconducting, whereas for Co doping the structural and magnetic transitions can be observed up to $x = 0.042$, and superconductivity occurs only for higher doping levels and with reduced transition temperatures. For dopings up to $x = 0.056$, we find evidence for short-range magnetic order. By means of relaxation-rate measurements, we map out the magnetic fluctuations that reveal the interplay of nematicity and magnetism. Above the nematic ordering, the spin fluctuations in LaFe_{1-x}Co_xAsO are identical to those in Ba(Fe_{1-x}Co_x)₂As₂, suggesting that nematicity in LaFeAsO is a result of the fluctuating spin density wave as well.

DOI: [10.1103/PhysRevB.103.L180506](https://doi.org/10.1103/PhysRevB.103.L180506)

The phase diagrams of unconventional superconductors are complex and reveal different, often competing phases. Antiferromagnetic order is the most common phase of parent compounds, which is destroyed by doping and followed by superconductivity. In iron pnictides, nematic order precedes the antiferromagnetic spin density wave (SDW) order, and there is a strong debate whether (i) spin fluctuations lead to a breaking of tetragonal symmetry and induce nematic order at T_S [1–9] or (ii) charge density fluctuations on the Fe d_{xz} and d_{yz} orbitals increase with decreasing temperature and lead to an unequal charge density distribution below T_S , i.e., to an orbital order [10–15]. Both magnetic and orbital fluctuations have been considered to serve as the pairing glue for superconductivity [6, 16–20]. One way to shed light on this problem is to compare orbital and spin fluctuations above T_S , as well as orbital order below T_S and SDW order below the magnetic transition temperature, T_N , in different families of iron pnictides. However, the lack of doped single crystals of the LaFeAsO family has prevented a full comparison with other iron pnictides or chalcogenides until recently [15]. Moreover, a comparison of different experimental techniques that probe different magnetic or electronic degrees of freedom such as spin or charge fluctuations is crucial in this context.

Here, we use nuclear magnetic resonance (NMR) to map out the magnetic fluctuations in LaFe_{1-x}Co_xAsO single crystals in order to reveal the interplay of nematicity and magnetism. We compare our data with results published for Co-doped BaFe₂As₂, FeSe, and polycrystalline F-doped LaFeAsO. The phase diagram of LaFe_{1-x}Co_xAsO agrees well with that of F-doped samples up to a nominal doping of $x = 0.03$. Above this level, the F-doped samples become superconducting, while the Co-doped samples still exhibit nematic and SDW order up to $x = 0.042$. Superconductivity

gradually sets in at 0.056, and 0.06 is the only concentration with bulk superconductivity. Contrasting the spin fluctuations measured by the spin-lattice relaxation rate, $(T_1T)^{-1}$, in LaFe_{1-x}Co_xAsO with those of Ba(Fe_{1-x}Co_x)₂As₂ shows that above T_S , $(T_1T)^{-1}$ is identical for samples with the same T_S . This indicates that the leading instability is towards a SDW in both compounds, in agreement with recent theoretical predictions [8, 9].

Co-doped single crystals of LaFeAsO were prepared by solid state crystal growth [21] and were characterized by x-ray diffraction, energy-dispersive x-ray spectroscopy (EDX), dilatometry, susceptibility, specific heat, and elastoresistivity [15, 22, 23]. The sample sizes were smaller than $1 \times 1 \times 0.1$ mm, and the maximal weight was about 0.3 mg. NMR has been measured on the ⁷⁵As nucleus for magnetic fields H oriented along $[100]_{\text{ortho}}$ (or $[010]_{\text{ortho}}$) and along $[001]$ (called a , b , and c). Due to the particular position of As in the crystal structure, ⁷⁵As NMR is an excellent probe of stripe-type spin fluctuations in iron pnictides, which can be measured by the spin-lattice relaxation rate and its anisotropy [24–35]. Furthermore, the NMR spectra split at the nematic ordering temperature due to an anisotropy of the Knight shift and of the electric quadrupole interaction and can thus distinguish the a and b directions in the orbital ordered state [13, 14, 30, 31, 34, 36–38].

In the upper row of Fig. 1 we show $(T_1T)^{-1}$. It increases at T_S even more rapidly than a Curie-Weiss fit $[(T_1T)^{-1} = a + C/(T - T_N)]$ to the data above T_S , and reaches a maximum at T_N . This behavior is the same for all samples that order long-range magnetically, i.e., up to $x = 0.042$, and indicates a critical slowing of stripe-type spin fluctuations towards the magnetically ordered SDW phase. It is also found in magnetically ordered F-doped polycrystals and in Ba(Fe_{1-x}Co_x)₂As₂

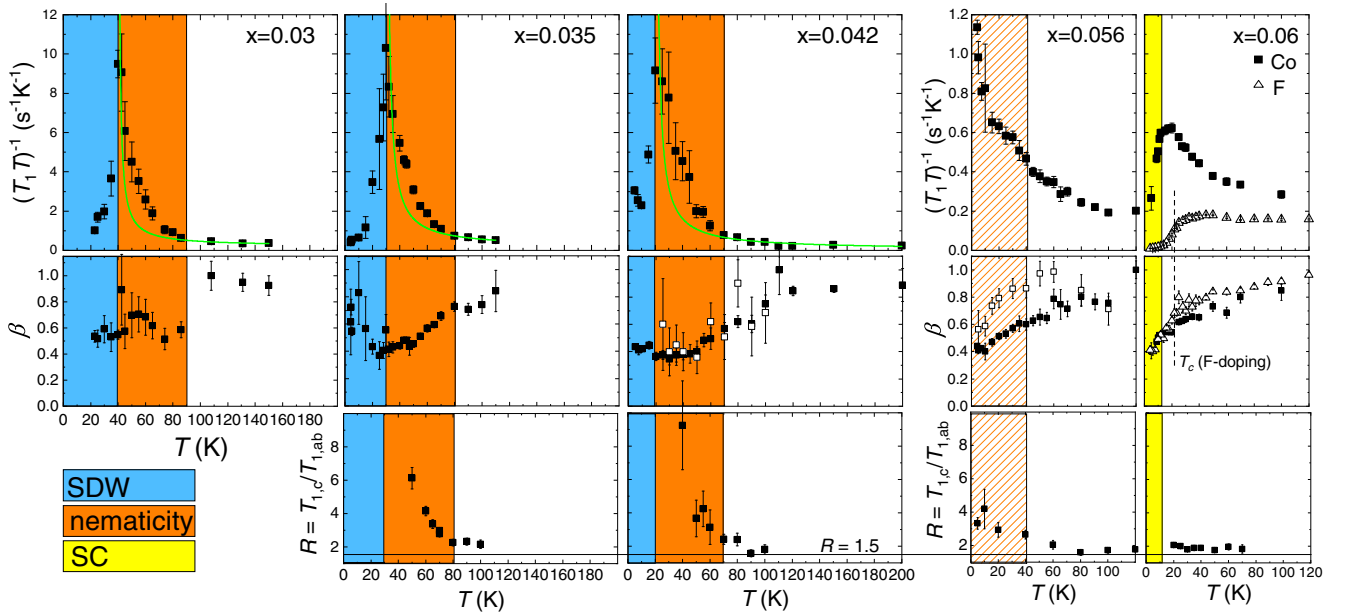


FIG. 1. Upper row: $(T_1T)^{-1}$ vs temperature with the magnetic field applied along the ab plane. In the last panel, $(T_1T)^{-1}$ of $x = 0.06$ F doping (open triangles) is included for comparison [35]. The y axis for $x = 0.056$ and $x = 0.06$ is ten times zoomed compared with the magnetically ordered samples. The green lines are Curie-Weiss fits with Θ fixed to T_N . Middle row: Stretching parameter β of T_1^{-1} ; open squares, stretching of the spin-spin relaxation rate T_2^{-1} . Lower row: Ratio $R = T_{1c}/T_{1ab}$. SC, superconductivity.

single crystals [27,29,35,39]. The maximum of $(T_1T)^{-1}$ has been taken as T_N , and the temperature where $(T_1T)^{-1}$ increases more rapidly than the Curie-Weiss fit defines T_S . These temperatures agree well with bulk measurements [15,23].

For $x = 0.056$, $(T_1T)^{-1}$ is strongly reduced and does not reach a maximum anymore, i.e., long-range magnetic order is absent. Note that the y axis in Fig. 1 is zoomed in by a factor of 10 for $x = 0.056$ and 0.06. Critical spin fluctuations above a potential magnetically ordered phase are definitely absent for these two doping levels. For $x = 0.056$, $(T_1T)^{-1}$ increases monotonically down to the lowest measured temperature. Yet, a slight change in slope is still visible at a temperature that would agree with a potential structural transition. For $x = 0.06$, $(T_1T)^{-1}$ goes through a broad maximum consistent with a glassy freezing of spin fluctuations at low temperatures without long-range magnetic order [35,40]. Below T_c , $(T_1T)^{-1}$ decreases rapidly due to the opening of the superconducting gap.

The middle row of Fig. 1 shows the stretching exponent, β , of the decay of the nuclear magnetization, which indicates a distribution of spin-lattice relaxation rates, where T_1^{-1} is the median of this distribution [41,42]. Stretched exponential relaxation often occurs in disordered systems and is present also for F doping [35,40] and in $\text{Ba}(\text{Fe}_{1-x}\text{Co}_x)_2\text{As}_2$ for doping levels above $x = 0.04$ [27,39,41]. It has been attributed to a coupling of the nematicity to random strain fields introduced by the Co dopants [29]. Our observation of an enhancement of the stretching at T_S for low Co concentrations ($x = 0.03$ and 0.035) seems to confirm this interpretation and is also consistent with the absence of stretching in $\text{Ba}(\text{Fe}_{1-x}\text{Co}_x)_2\text{As}_2$ for $x \leq 0.04$ [27], where the difference in temperature between T_S and T_N is much smaller. β reaches a minimum of about 0.4, indicating that the relaxation rate varies by several orders

of magnitude within a sample [42]. More sophisticated analyses of stretched relaxation to inspect the true distribution of T_1^{-1} [29,43] could not be performed here owing to the limited signal intensity of the small single crystals.

The lowermost row of Fig. 1 shows the ratio of $(T_1T)^{-1}$ measured for $H||ab$ and $H||c$, $R = T_{1ab}^{-1}/T_{1c}^{-1}$. Due to the peculiar hyperfine coupling of the ^{75}As nucleus, R is about 1.5 for isotropic spin fluctuations above T_S and becomes larger than 1.5 below T_S , where the spin fluctuations become anisotropic [24–26,28]. All samples that order long-range magnetically also show a clear change in R at the structural phase transition. The change in R for $x = 0.056$ is smoothed, indicating that a possible structural phase transition does not occur in the bulk of this sample. Finally, for $x = 0.06$, R is constant with temperature; that is, this sample is tetragonal down to the lowest T .

The NMR spectra are shown in Fig. 2 exemplarily for $x = 0.03, 0.042$, and 0.056 for $H||[100]_{\text{ortho}}$ or $[010]_{\text{ortho}}$. The spectra for $x = 0.035$ and 0.06 are shown in the Supplemental Material [44]. For all doping levels that exhibit a structural phase transition, the spectra broaden notably below T_S . Surprisingly, the spectra broaden at $T = 40$ K for $x = 0.056$, too, as can be seen in Fig. 3(a), where the full width at half maximum (FWHM) is plotted against temperature. The spectra of $x = 0.03$ even show remnants of a splitting, which indicates the anisotropy between the a and b directions due to the nematic transition [14,36]. For higher doping levels, the reduced orthorhombicity, $\delta = (a - b)/(a + b)$ [22], prevents resolving the splitting. Undoped LaFeAsO exhibits a splitting of about 75 kHz, which is already on the order of the FWHM for $x = 0.03$. The gradual increase in the linewidth at T_S is another determination method of the structural transition temperatures, which agree well with those determined

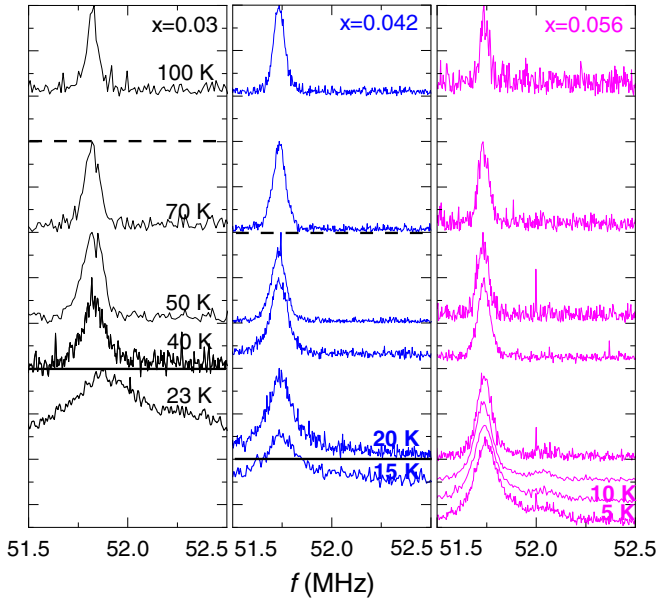


FIG. 2. NMR spectra for $x = 0.03$, 0.042 , and 0.056 for $H \parallel [100]_{\text{ortho}}$ or $[010]_{\text{ortho}}$. Solid lines mark T_N , and dashed lines mark T_S . For better visibility, spectra at low temperatures are enlarged. The excitation bandwidth is about 100 kHz for single-frequency scans; broader spectra were measured by a step-and-sum technique.

by $(T_1 T)^{-1}$. Note that for field orientation $H \parallel [110]_{\text{ortho}}$, the FWHM increases only moderately with decreasing temperature; see Fig. 3(a). For this orientation, the spectra of undoped LaFeAsO do not split below T_S [14]. The angular dependence of the linewidth below T_S can be used to confirm the correct orientation of the samples [44].

Below the SDW transition, the spectra shift to higher frequency and further broaden, indicating the existence of internal static hyperfine fields at the ^{75}As nuclei. The shift and broadening are typical for the field orientation $H \parallel ab$ [24]. With increasing doping, the hyperfine field quickly decreases [27]. The shift and broadening are therefore best visible for the lowest doping level of $x = 0.03$ in Fig. 2. In addition, the spectra develop a shoulder at even higher frequency, indicating that some nuclei feel higher internal magnetic fields. Interestingly, such a shoulder is also visible for $x = 0.056$ below about 20 K and indicates that at least parts of this sample develop static magnetism as well.

Another feature of the spectra is a loss of signal intensity about 15–20 K above the magnetic ordering temperature. Such a wipeout of signal intensity is also present in $\text{Ba}(\text{Fe}_{1-x}\text{Co}_x)_2\text{As}_2$, and has been ascribed to a shortening of the spin-lattice and spin-spin relaxation rates and their distribution over a few orders of magnitude [29,41]. This is known as a dynamic wipeout, where the nuclei relax so fast that they cannot be observed anymore. Our $(T_1 T)^{-1}$ and β values for $x = 0.03$, 0.035 , and 0.042 are very close to those observed in underdoped BaFe_2As_2 , and therefore a shortening of relaxation times seems to be the main reason for wipeout in underdoped $\text{LaFe}_{1-x}\text{Co}_x\text{AsO}$. However, the intensity decreases for $x = 0.056$ below about 20 K, too, despite the fact that $(T_1 T)^{-1}$ is about ten times smaller for this sample.

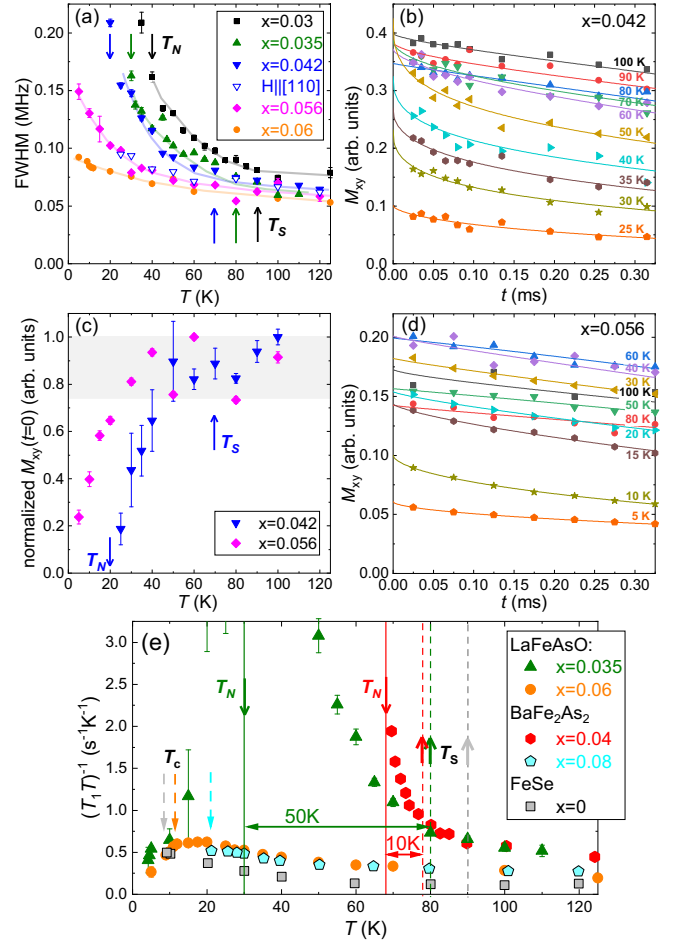


FIG. 3. (a) FWHM for all doping levels for $H \parallel [100]$ or $[010]$. Open symbols are for $H \parallel [110]$. (b) Spin-spin decay of the nuclear magnetization M_{xy} for $x = 0.042$. (c) M_{xy} at $t = 0$ s vs temperature for $x = 0.042$ and $x = 0.056$. (d) Spin-spin decay for $x = 0.056$. (e) $(T_1 T)^{-1}$ for $\text{LaFe}_{1-x}\text{Co}_x\text{AsO}$ with $x = 0.035$ and $x = 0.06$, for $\text{Ba}(\text{Fe}_{1-x}\text{Co}_x)_2\text{As}_2$ with $x = 0.04$ and $x = 0.08$ [45] and for FeSe [13]. Solid down arrows indicate T_N , dashed-down arrows indicate T_c , and up arrows indicate T_S .

To further investigate the development of magnetism in the nematic phase, we measured the spin-spin relaxation rate for $x = 0.042$ and $x = 0.056$, i.e., at the border between long-range magnetic order and superconductivity. The decay of the in-plane nuclear magnetization M_{xy} is plotted in Figs. 3(b) and 3(d). M_{xy} was fit globally at all temperatures for a given sample to a combined exponential and Gaussian form: $M_{xy}(t) = M_0 \exp[-(2t/T_2)^\beta] \exp[-(2t)^2/2T_{2G}^2]$, where M_0 is the initial nuclear magnetization, and t is the time between the 90° and 180° pulses. T_2 is the exponential spin-spin relaxation time, and T_{2G} is the Gaussian relaxation time, which turned out not to be temperature dependent [29,35,44,46].

$\beta \leq 1$ accounts for a distribution of spin-spin relaxation times similar to the distribution of the spin-lattice relaxation times. Yet, in contrast to T_1 , β affects mostly the first few tens of microseconds of the T_2 relaxation, which is the time slot that is most difficult to measure due to ringing of the resonance circuit, especially for such small samples as have been measured here [47]. β of T_2 is shown in the middle

row of Fig. 1 in comparison to β of T_1 . For $x = 0.042$, both β show approximately the same temperature dependence, whereas for $x = 0.056$, $\beta(T_1)$ is notably smaller than $\beta(T_2)$. However, both data sets in Figs. 3(b) and 3(d) clearly show that, even considering a stretching, $M_{xy}(t = 0)$ decreases with decreasing temperature [see Fig. 3(c)]. This is evidence for the presence of local static magnetic fields below about $T_{\text{SRO}} = 42$ K for $x = 0.042$ and below about $T_{\text{SRO}} = 23$ K for $x = 0.056$, in contrast to the mostly dynamic wipeout observed in $\text{Ba}(\text{Fe}_{1-x}\text{Co}_x)_2\text{As}_2$. These static magnetic fields shift a part of the resonance out of the detection bandwidth of a relaxation measurement, which was about 100 kHz. Static short-range magnetism has also been found in F-doped LaFeAsO polycrystals below T_S and has been attributed to a nanoscale phase separation in doped LaFeAsO [35,48], which we found for Co-doped polycrystals as well [49].

A comparison of low-frequency spin fluctuations above T_S with those in $\text{Ba}(\text{Fe}_{1-x}\text{Co}_x)_2\text{As}_2$ reveals whether the nematic order is driven by magnetic fluctuations or by orbital order [4,9]. Figure 3(e) shows $(T_1T)^{-1}$ for two samples for each of the different families, which have similar structural transition temperatures, namely, for $\text{Ba}(\text{Fe}_{1-x}\text{Co}_x)_2\text{As}_2$ with $x = 0.04$ from Ref. [27] and for $\text{LaFe}_{1-x}\text{Co}_x\text{AsO}$ with $x = 0.035$ from this work. The relaxation rates for these two samples are identical above T_S . Below T_S , $(T_1T)^{-1}$ increases much faster with decreasing temperature for $\text{Ba}(\text{Fe}_{1-x}\text{Co}_x)_2\text{As}_2$. This is also true for the undoped samples except for a constant offset, if the temperature is normalized by T_S [44]. Differences in spin fluctuations therefore appear only below T_S , possibly caused by a stronger coupling of nematicity and magnetism in BaFe_2As_2 compared with LaFeAsO , in agreement with the smaller difference of T_S and T_N in BaFe_2As_2 . For optimal doping levels which do not exhibit a structural transition, $(T_1T)^{-1}$ is again identical for both compounds down to the superconducting transition temperature T_c [see Fig. 3(e)]. In contrast, $(T_1T)^{-1}$ of FeSe is even smaller than that of optimally doped LaFeAsO and BaFe_2As_2 , even below T_S [50]. Here, the coupling of nematicity and magnetism is even weaker, so that no strong enhancement of low-frequency spin fluctuations appears, either above or below T_S , and no static magnetism develops despite the nematic order at $T_S = 90$ K. These results suggest that the leading instability for LaFeAsO and BaFe_2As_2 is the SDW in agreement with recent theoretical considerations [8,9]. In contrast, FeSe shows a different, possibly spin-orbital-intertwined nematic order without the typical magnetic fluctuations that can be probed at the position of the Se (or As) nucleus [13,51,52].

All results can be combined in the phase diagram in Fig. 4. Up to $x = 0.03$ the phase diagram for Co doping coincides with F-doped polycrystals, and T_S and T_N decrease linearly with doping. Above $x = 0.03$, F-doped samples become superconducting, and nematicity and magnetism disappear abruptly, whereas for Co doping, T_S and T_N can still be detected up to $x = 0.042$. The sample with $x = 0.056$ shows remnants of a structural transition [see Figs. 1 and 3(a)] and short-range magnetic order below $T_{\text{SRO}} \approx 23$ K. This is the first doping that exhibits superconductivity, albeit with a reduced volume fraction and only in low magnetic fields [superconducting quantum interference device (SQUID)].

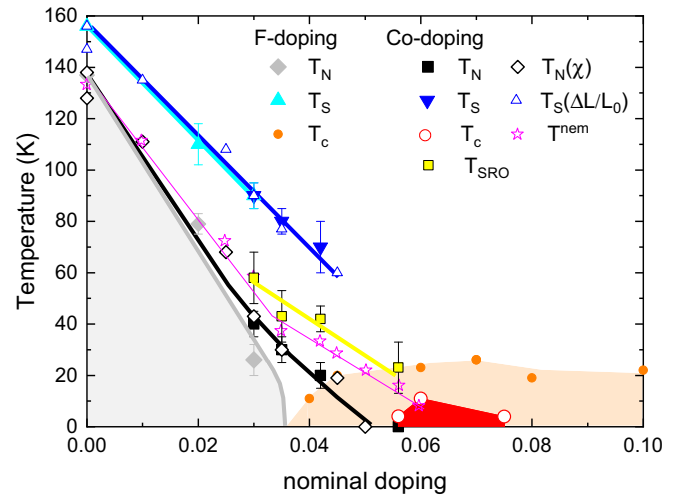


FIG. 4. Phase diagram resulting from NMR and SQUID susceptibility on Co-doped LaFeAsO single crystals compared with F-doped polycrystals [35]. Closed symbols are from NMR, and open symbols are from SQUID and dilatometry [23]. T^{nem} is determined by elasto-resistivity [15].

Finally, $x = 0.06$ is the only doping with bulk superconductivity and absence of nematicity and magnetism [23]. Compared with Co-doped BaFe_2As_2 , T_N and T_S decrease much faster with doping in LaFeAsO , which is surprising considering the larger superconducting range for BaFe_2As_2 and the higher T_c 's. This could be a consequence of a nanoscale electronic phase separation in LaFeAsO [35], where doping leads to a percolation of the magnetic square lattice and therefore to a more effective suppression of nematicity and magnetism. In contrast, superconductivity and magnetism can coexist in Co-doped BaFe_2As_2 , and no phase separation occurs. However, the spin fluctuations are very similar in both compounds and are not affected by the electronic phase separation [48]. Interestingly, the nematic transition temperature T^{nem} determined by elasto-resistivity measurements on the same $\text{LaFe}_{1-x}\text{Co}_x\text{AsO}$ crystals [15] follows the short-range magnetic order temperature determined here, indicating that nematicity could be related to magnetism even for larger Co contents in LaFeAsO .

In conclusion, we show that spin fluctuations determined by NMR above the nematic ordering temperature are identical in $\text{LaFe}_{1-x}\text{Co}_x\text{AsO}$ and $\text{Ba}(\text{Fe}_{1-x}\text{Co}_x)_2\text{As}_2$. There is strong evidence that spin fluctuations drive nematicity in $\text{Ba}(\text{Fe}_{1-x}\text{Co}_x)_2\text{As}_2$ [4]. Therefore we speculate that nematicity is a result of the fluctuating SDW order in $\text{LaFe}_{1-x}\text{Co}_x\text{AsO}$ as well. Recent theoretical work showed that the leading instability is towards a SDW in LaFeAsO and BaFe_2As_2 , whereas the leading instability in FeSe is orbital order [8,9]. Indeed, the spin fluctuations measured by $(T_1T)^{-1}$ in FeSe are much weaker, consistent with the theoretical results. Furthermore, the short-range magnetic ordering revealed by NMR could be responsible for the anomalous doping dependence of T^{nem} determined recently by elasto-resistivity [15]. Therefore we believe that nematicity is driven by spin fluctuations in Co-doped LaFeAsO for all doping levels.

We would like to thank Rüdiger Klingeler, Christian Hess, and Xiaochen Hong for helpful discussions. This work has been supported by the Deutsche Forschungsgemeinschaft (DFG) through Grants No. AS 523/4-1 and No. DI2538/1-1,

the research training group GRK1621, through SFB 1143 (Project No. 247310070), and the Würzburg-Dresden Cluster of Excellence on Complexity and Topology in Quantum Matter ct.qmat (EXC 2147, Project No. 390858490).

- [1] C. Fang, H. Yao, W.-F. Tsai, J. P. Hu, and S. A. Kivelson, Theory of electron nematic order in LaFeAsO, *Phys. Rev. B* **77**, 224509 (2008).
- [2] C. Xu, M. Müller, and S. Sachdev, Ising and spin orders in the iron-based superconductors, *Phys. Rev. B* **78**, 020501(R) (2008).
- [3] I. Paul, Magnetoelastic Quantum Fluctuations and Phase Transitions in the Iron Superconductors, *Phys. Rev. Lett.* **107**, 047004 (2011).
- [4] R. M. Fernandes, A. E. Böhm, C. Meingast, and J. Schmalian, Scaling between Magnetic and Lattice Fluctuations in Iron Pnictide Superconductors, *Phys. Rev. Lett.* **111**, 137001 (2013).
- [5] X. Y. Lu, J. T. Park, R. Zhang, H. Q. Luo, A. H. Nevidomskyy, Q. M. Si, and P. C. Dai, Nematic spin correlations in the tetragonal state of uniaxial-strained BaFe_{2-x}Ni_xAs₂, *Science* **345**, 657 (2014).
- [6] R. M. Fernandes, A. V. Chubukov, and J. Schmalian, What Drives Nematic Order in Fe-Based Superconductors?, *Nat. Phys.* **10**, 97 (2014).
- [7] F. Kretzschmar, T. Böhm, U. Karahasanović, B. Muschler, A. Baum, D. Jost, J. Schmalian, S. Caprara, M. Grilli, C. Di Castro, J. G. Analytis, J.-H. Chu, I. R. Fisher, and R. Hackl, Critical scaraspin fluctuations and the origin of nematic order in Ba(Fe_{1-x}Co_x)₂As₂, *Nat. Phys.* **12**, 560 (2016).
- [8] Y. Yamakawa, S. Onari, and H. Kontani, Nematicity and Magnetism in FeSe and Other Families of Fe-Based Superconductors, *Phys. Rev. X* **6**, 021032 (2016).
- [9] A. V. Chubukov, M. Khodas, and R. M. Fernandes, Magnetism, Superconductivity, and Spontaneous Orbital Order in Iron-Based Superconductors: Which Comes First and Why?, *Phys. Rev. X* **6**, 041045 (2016).
- [10] C.-C. Lee, W. G. Yin, and W. Ku, Ferro-Orbital Order and Strong Magnetic Anisotropy in the Parent Compounds of Iron-Pnictide Superconductors, *Phys. Rev. Lett.* **103**, 267001 (2009).
- [11] C.-C. Chen, J. Maciejko, A. P. Sorini, B. Moritz, R. R. P. Singh, and T. P. Devereaux, Orbital order and spontaneous orthorhombicity in iron pnictides, *Phys. Rev. B* **82**, 100504(R) (2010).
- [12] H. Kontani and S. Onari, Orbital-Fluctuation-Mediated Superconductivity in Iron Pnictides: Analysis of the Five-Orbital Hubbard-Holstein Model, *Phys. Rev. Lett.* **104**, 157001 (2010).
- [13] S.-H. Baek, D. V. Efremov, J. M. Ok, J. S. Kim, J. van den Brink, and B. Büchner, Orbital-driven nematicity in FeSe, *Nat. Mat.* **14**, 210 (2014).
- [14] J. M. Ok, S.-H. Baek, D. V. Efremov, R. Kappenberger, S. Aswartham, J. S. Kim, J. van den Brink, and B. Büchner, Nematicity and magnetism in LaFeAsO single crystals probed by ⁷⁵As nuclear magnetic resonance, *Phys. Rev. B* **97**, 180405(R) (2018).
- [15] X. Hong, F. Caglieris, R. Kappenberger, S. Wurmehl, S. Aswartham, F. Scaravaggi, P. Lepucki, A. U. B. Wolter, H.-J. Grafe, B. Büchner, and C. Hess, Evolution of the Nematic Susceptibility in LaFe_{1-x}Co_xAsO, *Phys. Rev. Lett.* **125**, 067001 (2020).
- [16] I. I. Mazin, D. J. Singh, M. D. Johannes, and M. H. Du, Unconventional Superconductivity with a Sign Reversal in the Order Parameter of LaFeAsO_{1-x}F_x, *Phys. Rev. Lett.* **101**, 057003 (2008).
- [17] K. Kuroki, S. Onari, R. Arita, H. Usui, Y. Tanaka, H. Kontani, and H. Aoki, Unconventional Pairing Originating from the Disconnected Fermi Surfaces of Superconducting LaFeAsO_{1-x}F_x, *Phys. Rev. Lett.* **101**, 087004 (2008).
- [18] S. Lederer, Y. Schattner, E. Berg, and S. A. Kivelson, Enhancement of Superconductivity near a Nematic Quantum Critical Point, *Phys. Rev. Lett.* **114**, 097001 (2015).
- [19] M. A. Metlitski, D. F. Mross, S. Sachdev, and T. Senthil, Cooper pairing in non-Fermi liquids, *Phys. Rev. B* **91**, 115111 (2015).
- [20] D. Labat and I. Paul, Pairing instability near a lattice influenced nematic quantum critical point, *Phys. Rev. B* **96**, 195146 (2017).
- [21] R. Kappenberger, S. Aswartham, F. Scaravaggi, C. G. F. Blum, M. I. Sturza, A. U. B. Wolter, S. Wurmehl, and B. Büchner, Solid state single crystal growth of three-dimensional faceted LaFeAsO crystals, *J. Cryst. Growth* **483**, 9 (2018).
- [22] L. Wang, S. Sauerland, F. Scaravaggi, R. Kappenberger, S. Aswartham, S. Wurmehl, A. U. B. Wolter, B. Büchner, and R. Klingeler, Nematicity and structure in LaFe_{1-x}Co_xAsO, *J. Magn. Magn. Mater.* **482**, 50 (2019).
- [23] F. Scaravaggi, S. Sauerland, L. Wang, R. Kappenberger, P. Lepucki, A. P. Dioguardi, C. Wuttke, X. Hong, C. Hess, H.-J. Grafe, S. Wurmehl, S. Aswartham, R. Klingeler, A. U. B. Wolter, and B. Büchner, Revisiting the phase diagram of LaFe_{1-x}Co_xAsO single crystals by thermodynamic methods, *Phys. Rev. B* **103**, 174506 (2021).
- [24] K. Kitagawa, N. Katayama, K. Ohgushi, and M. Takigawa, Antiferromagnetism of SrFe₂As₂ studied by single-crystal ⁷⁵As-NMR, *J. Phys. Soc. Jpn.* **78**, 063706 (2009).
- [25] S. Kitagawa, Y. Nakai, T. Iye, K. Ishida, Y. Kamihara, M. Hirano, and H. Hosono, Stripe antiferromagnetic correlations in LaFeAsO_{1-x}F_x probed by ⁷⁵As NMR, *Phys. Rev. B* **81**, 212502 (2010).
- [26] Y. Nakai, S. Kitagawa, T. Iye, K. Ishida, Y. Kamihara, M. Hirano, and H. Hosono, Enhanced anisotropic spin fluctuations below tetragonal-to-orthorhombic transition in LaFeAs(O_{1-x}F_x) probed by ⁷⁵As and ¹³⁹La NMR, *Phys. Rev. B* **85**, 134408 (2012).
- [27] F. L. Ning, M. Fu, D. A. Torchetti, T. Imai, A. S. Sefat, P. Cheng, B. Shen, and H.-H. Wen, Critical behavior of the spin density wave transition in underdoped Ba(Fe_{1-x}Co_x)₂As₂ (x ≤ 0.05): ⁷⁵As NMR investigation, *Phys. Rev. B* **89**, 214511 (2014).
- [28] H.-J. Grafe, U. Gräfe, A. P. Dioguardi, N. J. Curro, S. Aswartham, S. Wurmehl, and B. Büchner, Identical spin fluctuations in Cu- and Co-doped BaFe₂As₂ independent of electron doping, *Phys. Rev. B* **90**, 094519 (2014).
- [29] A. P. Dioguardi, M. M. Lawson, B. T. Bush, J. Crocker, K. R. Shirer, D. M. Nisson, T. Kissikov, S. Ran, S. L. Bud'ko, P. C. Canfield, S. Yuan, P. L. Kuhns, A. P. Reyes, H.-J. Grafe, and N. J. Curro, NMR evidence for inhomogeneous glassy behavior

- driven by nematic fluctuations in iron arsenide superconductors, *Phys. Rev. B* **92**, 165116 (2015).
- [30] A. E. Böhmer, T. Arai, F. Hardy, T. Hattori, T. Iye, T. Wolf, H. v. Löhneysen, K. Ishida, and C. Meingast, Origin of the Tetragonal-to-Orthorhombic Phase Transition in FeSe: A Combined Thermodynamic and NMR Study of Nematicity, *Phys. Rev. Lett.* **114**, 027001 (2015).
- [31] R. Zhou, L. Y. Xing, X. C. Wang, C. Q. Jin, and G.-q. Zheng, Orbital order and spin nematicity in the tetragonal phase of the electron-doped iron pnictides $\text{NaFe}_{1-x}\text{Co}_x\text{As}$, *Phys. Rev. B* **93**, 060502(R) (2016).
- [32] T. Kissikov, R. Sarkar, M. Lawson, B. T. Bush, E. I. Timmons, M. A. Tanatar, R. Prozorov, S. L. Bud'ko, P. C. Canfield, R. M. Fernandes, and N. J. Curro, Uniaxial strain control of spin-polarization in multicomponent nematic order of BaFe_2As_2 , *Nat. Commun.* **9**, 1058 (2018).
- [33] Z. T. Zhang, D. Dmytriieva, S. Molatta, J. Wosnitzer, S. Khim, S. Gass, A. U. B. Wolter, S. Wurmehl, H.-J. Grafe, and H. Kühne, Increasing stripe-type fluctuations in AFe_2As_2 ($A = \text{K}, \text{Rb}, \text{Cs}$) superconductors probed by ^{75}As NMR spectroscopy, *Phys. Rev. B* **97**, 115110 (2018).
- [34] S.-H. Baek, J. M. Ok, J. S. Kim, S. Aswartham, I. Morozov, D. Chareev, T. Urata, K. Tanigaki, Y. Tanabe, B. Büchner, and D. V. Efremov, Separate tuning of nematicity and spin fluctuations to unravel the origin of superconductivity in FeSe, *npj Quantum Mater.* **5**, 8 (2020).
- [35] H.-J. Grafe, P. Lepucki, M. Witschel, A. P. Dioguardi, R. Kappenberger, S. Aswartham, S. Wurmehl, and B. Büchner, Unified phase diagram of F-doped LaFeAsO by means of NMR and NQR parameters, *Phys. Rev. B* **101**, 054519 (2020).
- [36] M. Fu, D. A. Torchetti, T. Imai, F. L. Ning, J.-Q. Yan, and A. S. Sefat, NMR Search for the Spin Nematic State in a LaFeAsO Single Crystal, *Phys. Rev. Lett.* **109**, 247001 (2012).
- [37] M. Toyoda, A. Ichikawa, Y. Kobayashi, M. Sato, and M. Itoh, In-plane anisotropy of the electric field gradient in $\text{Ba}(\text{Fe}_{1-x}\text{Co}_x)_2\text{As}_2$ observed by ^{75}As NMR, *Phys. Rev. B* **97**, 174507 (2018).
- [38] M. Toyoda, Y. Kobayashi, and M. Itoh, Nematic fluctuations in iron arsenides NaFeAs and LiFeAs probed by ^{75}As NMR, *Phys. Rev. B* **97**, 094515 (2018).
- [39] T. Kissikov, A. P. Dioguardi, E. I. Timmons, M. A. Tanatar, R. Prozorov, S. L. Bud'ko, P. C. Canfield, R. M. Fernandes, and N. J. Curro, NMR study of nematic spin fluctuations in a detwinned single crystal of underdoped $\text{Ba}(\text{Fe}_{1-x}\text{Co}_x)_2\text{As}_2$, *Phys. Rev. B* **94**, 165123 (2016).
- [40] F. Hammerath, U. Gräfe, T. Kühne, H. Kühne, P. L. Kuhns, A. P. Reyes, G. Lang, S. Wurmehl, B. Büchner, P. Carretta, and H.-J. Grafe, Progressive slowing down of spin fluctuations in underdoped $\text{LaFeAsO}_{1-x}\text{F}_x$, *Phys. Rev. B* **88**, 104503 (2013).
- [41] A. P. Dioguardi, J. Crocker, A. C. Shockley, C. H. Lin, K. R. Shirer, D. M. Nisson, M. M. Lawson, N. apRoberts-Warren, P. C. Canfield, S. L. Bud'ko, S. Ran, and N. J. Curro, Coexistence of Cluster Spin Glass and Superconductivity in $\text{BaFe}(\text{Fe}_{1-x}\text{Co}_x)_2\text{As}_2$ for $0.06 \leq x \leq 0.071$, *Phys. Rev. Lett.* **111**, 207201 (2013).
- [42] D. C. Johnston, Stretched exponential relaxation arising from a continuous sum of exponential decays, *Phys. Rev. B* **74**, 184430 (2006).
- [43] P. M. Singer, A. Arsenault, T. Imai, and M. Fujita, ^{139}La NMR investigation of the interplay between lattice, charge, and spin dynamics in the charge-ordered high- T_c cuprate $\text{La}_{1.875}\text{Ba}_{0.125}\text{CuO}_4$, *Phys. Rev. B* **101**, 174508 (2020).
- [44] See Supplemental Material at <http://link.aps.org/supplemental/10.1103/PhysRevB.103.L180506> for spectra for $x = 0.035$ and 0.06 , Knight shift, T_2 , angular dependence of the FWHM for $x = 0.042$, and a detailed comparison with $\text{Ba}(\text{Fe}_{1-x}\text{Co}_x)_2\text{As}_2$, which includes Refs. [53–55].
- [45] F. L. Ning, K. Ahilan, T. Imai, A. S. Sefat, M. A. McGuire, B. C. Sales, D. Mandrus, P. Cheng, B. Shen, and H.-H. Wen, Contrasting Spin Dynamics between Underdoped and Overdoped $\text{Ba}(\text{Fe}_{1-x}\text{Co}_x)_2\text{As}_2$, *Phys. Rev. Lett.* **104**, 037001 (2010).
- [46] L. Bossoni, P. Carretta, W. P. Halperin, S. Oh, A. Reyes, P. Kuhns, and P. C. Canfield, Evidence of unconventional low-frequency dynamics in the normal phase of $\text{Ba}(\text{Fe}_{1-x}\text{Rh}_x)_2\text{As}_2$ iron-based superconductors, *Phys. Rev. B* **88**, 100503(R) (2013).
- [47] D. Pelc, H.-J. Grafe, G. D. Gu, and M. Požek, Cu nuclear magnetic resonance study of charge and spin stripe order in $\text{La}_{1.875}\text{Ba}_{0.125}\text{CuO}_4$, *Phys. Rev. B* **95**, 054508 (2017).
- [48] G. Lang, H.-J. Grafe, D. Paar, F. Hammerath, K. Manthey, G. Behr, J. Werner, and B. Büchner, Nanoscale Electronic Order in Iron Pnictides, *Phys. Rev. Lett.* **104**, 097001 (2010).
- [49] P. Lepucki, A. P. Dioguardi, R. Havemann, R. Kappenberger, S. Wurmehl, S. Aswartham, B. Büchner, and H.-J. Grafe, NQR measurements of $\text{LaFe}_{1-x}\text{Co}_x\text{AsO}$ polycrystals (unpublished).
- [50] In FeSe, $(T_1T)^{-1}$ has been measured in a magnetic field of 9 T on the ^{77}Se nucleus, which has a slightly different gyromagnetic ratio. This leads to a reduction of $(T_1T)^{-1}$ by at most 15% compared with our ^{75}As NMR on doped LaFeAsO in 7 T. This alone cannot explain the 100% smaller $(T_1T)^{-1}$ in FeSe compared with optimally doped LaFeAsO .
- [51] J. Li, B. Lei, D. Zhao, L. P. Nie, D. W. Song, L. X. Zheng, S. J. Li, B. L. Kang, X. G. Luo, T. Wu, and X. H. Chen, Spin-Orbital-Intertwined Nematic State in FeSe, *Phys. Rev. X* **10**, 011034 (2020).
- [52] R. Zhou, D. D. Scherer, H. Mayaffre, P. Toulemonde, M. Ma, Y. Li, B. M. Andersen, and M.-H. Julien, Singular magnetic anisotropy in the nematic phase of FeSe, *npj Quantum Mater.* **5**, 93 (2020).
- [53] H.-J. Grafe, D. Paar, G. Lang, N. J. Curro, G. Behr, J. Werner, J. Hamann-Borrero, C. Hess, N. Leps, R. Klingeler, and B. Büchner, ^{75}As NMR Studies of Superconducting $\text{LaFeAsO}_{0.9}\text{F}_{0.1}$, *Phys. Rev. Lett.* **101**, 047003 (2008).
- [54] K. Kitagawa, N. Katayama, K. Ohgushi, M. Yoshida, and M. Takigawa, Commensurate itinerant antiferromagnetism in BaFe_2As_2 : ^{75}As -NMR studies on a self-flux grown single crystal, *J. Phys. Soc. Jpn.* **77**, 114709 (2008).
- [55] S. Nandi, M. G. Kim, A. Kreyssig, R. M. Fernandes, D. K. Pratt, A. Thaler, N. Ni, S. L. Bud'ko, P. C. Canfield, J. Schmalian, R. J. McQueeney, and A. I. Goldman, Anomalous Suppression of the Orthorhombic Lattice Distortion in Superconducting $\text{BaFe}_{2-x}\text{Co}_x\text{As}_2$ Single Crystals, *Phys. Rev. Lett.* **104**, 057006 (2010).